

# Full Bridge Three-Port Converters for Solar Power Systems

Riya Anto<sup>1</sup>, Bindukala M. P<sup>2</sup>

Department of EEE, Nehru College of Engineering and Research Centre, Thrissur, India

**Abstract:** A Three Port Converter (TPC), which can interface with renewable sources, storage elements and loads simultaneously, is a good candidate for the solar power systems. My aim is to produce constant output power in all times (day & night). So I used three port full bridge converters in solar electrical energy. A systematic method for generating Three Port Converter topologies from Full Bridge Converters are described here. By using this systematic method, a novel full-bridge TPC (FB-TPC) is developed for renewable power system applications which feature simple topologies and control, a reduced number of devices and single-stage power conversion between any two of the three ports. This method splits the two switching legs of the FBC into two switching cells with different sources and allows a dc bias current in the transformer. The FB-TPC consists of two bidirectional ports and an isolated output port. The primary circuit of the converter functions as a buck-boost converter and provides a power flow path between the ports on the primary side, while the third port provides the power balance in the system ports. The full bridge three port converter is designed and simulated using MATLAB/SIMULINK. The output parameters such as output voltage, current and power were obtained.

**Keywords:** Boost-buck, dc-dc converter, full-bridge converter (FBC), renewable power system, three-port converter (TPC)

## 1. Introduction

Renewable power systems, which are capable of harvesting energy from, for example, solar cells, fuel cells, wind, and thermoelectric generators, are found in many applications such as hybrid electric vehicles, satellites, traffic lights, and powering remote communication systems. Since the output power of renewable sources is stochastic and the sources lack energy storage capabilities, energy storage systems such as a battery or a supercapacitor are required to improve the system dynamics and steady-state characteristics. A three-port converter (TPC), which can interface with renewable sources, storage elements, and loads, simultaneously, is a good candidate for a renewable power system [1]-[9].

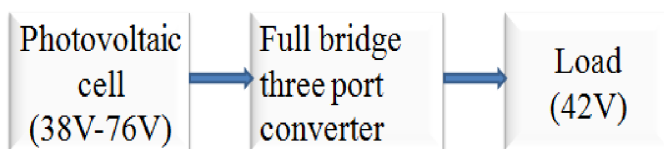


Figure 1: Block Diagram

Different topologies like multiport converters [4], multiport power electric interface [2] etc. are done by researchers earlier. But this is not an integrated solution since only a few devices are shared. Some TPCs are constructed from full-bridge, half-bridge, or series-resonant topologies by utilizing the magnetic coupling through a multiwinding transformer [8]-[9]. However, too many active switches have been used, resulting in a complicated driving and control circuit, which may degrade the reliability and performance of the integrated converters. Some three port converters like boost-integrated TPC [10] developed from a phase-shift full-bridge converter (FBC) and a buck integrated TPC [5]-[7] from a half-bridge

converter is to implement three-port interface. However, because the equivalent conversion circuit between the input source and energy storage element is a step-up or step-down converter with limited voltage conversion ratio, they are not flexible enough for applications where the voltage of the source port, such as solar, fuel cells and thermoelectric generator, varies over a wide range. We focus on full bridge three port converter which is buck boost integrated for both buck and boost operations. It uses fewer components thereby achieves higher system efficiency.

A three port converter must features single-stage conversion between any two of the three ports, higher system efficiency, fewer components, faster response, compact packaging, and unified power management among the ports with centralized control. For renewable energy harvesting systems, one of the toughest challenges for the power management circuits is that, the converter must be able to efficiently function with challenging wide source voltage conditions. This motivates the need of buck-boost integrated full bridge three port converters with wide input voltage range, higher system efficiency, and small physical size. ZVS of all the primary-side switches can also be achieved with this FB-TPC.

In Section II, the basic ideas used to generate FB-TPC are given. In Section III, the FB-TPC is analyzed, with operation principles and design considerations. Simulation results are given in Section IV. Finally, conclusions will be given in Section V.

## 2. Derivation OF The FB-TPC From a Full-Bridge DC-DC Converter

A systematic method for generating Three Port Converter topologies from Full Bridge Converters are described here. This systematic method is used to find a novel full bridge TPC (FB-TPC). This method splits the two switching legs of the FBC into two switching cells with different sources and allows a dc bias current in the transformer. A buck boost converter is integrated in the FB-TPC and used to configure the power flow path between the two ports on the primary side of the converter, which is aimed to handle a wide range of source voltage. ZVS of all the primary-side switches can also be achieved with this FB-TPC.

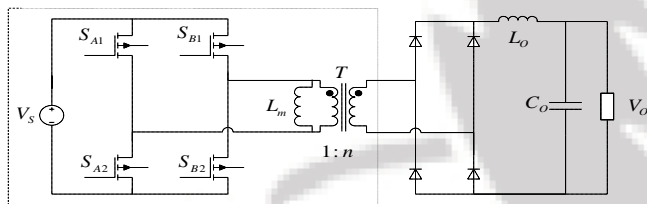


Figure 2: Full Bridge Converter

Referring to Fig.2, the primary side of the FBC consists of two switching legs, composed of  $S_{A1}$ ,  $S_{A2}$  and  $S_{B1}$ ,  $S_{B2}$  in parallel, connected to a common input source  $V_s$ . For the primary side of the FBC, the constraint condition of the operation of the FBC is the voltage-second balance principle of the magnetizing inductor  $L_m$ . This means that, from a topological point of view, the two switching legs of the FBC can also be split into two symmetrical parts, cells A and B, if only  $L_m$  satisfies the voltage-second balance principle, as shown in Fig.3.

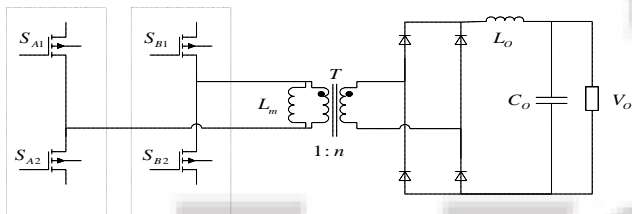


Figure 3: Two Switching Cells of Full Bridge Converter

The two cells can be connected to different sources,  $V_{sa}$  &  $V_{sb}$  respectively, as shown in Fig.4, and then a novel FB-TPC is derived. The voltage of the two sources of the FB-TPC can be arbitrary. Specially, if  $V_{sa}$  always equals  $V_{sb}$ , the two cells can be paralleled directly and then the conventional FBC is derived. Therefore, the FBC can be seen as a special case of the FB-TPC as shown in Fig.4.

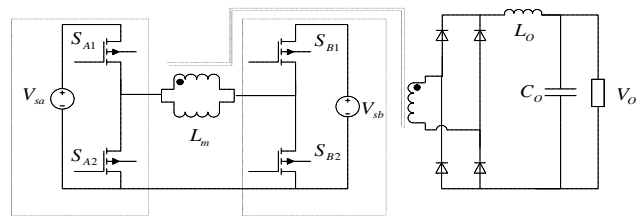


Figure 4: Full Bridge Three Port Converter

Close observation indicates that the FB-TPC has a symmetrical structure and both  $V_{sa}$  and  $V_{sb}$  can supply power to the load  $V_o$ . In addition, a bidirectional buck-boost converter [11] is also integrated in the primary side of the FB-TPC by employing the magnetizing inductor of the transformer  $L_m$  as a filter inductor. With the bidirectional buck-boost converter, the power flow paths between the two sources,  $V_{sa}$  and  $V_{sb}$ , can be configured and the power can be transferred between  $V_{sa}$  and  $V_{sb}$  freely. The unique characteristics of the FB-TPC are analyzed and summarized as follows.

- 1) The FB-TPC has two bidirectional ports and one isolated output port. Single-stage power conversion between any two of the three ports is achieved. The FB-TPC is suitable for renewable power systems and can be connected with an input source and an energy storage element, such as the photovoltaic (PV) with a battery backup or with two energy storage elements, such as the hybrid battery and the supercapacitor power system.
- 2) A buck-boost converter is integrated in the primary side of the FB-TPC. With the integrated converter, the source voltage  $V_{sa}$  can be either higher or lower than  $V_{sb}$  and vice versa. This indicates that the converter allows the sources voltage varies over a wide range.
- 3) The devices of the FB-TPC are the same as the FBC and no additional devices are introduced which means high integration is achieved.
- 4) All four active switches in the primary side of the FB TPC can be operated with ZVS by utilizing the energy stored in the leakage inductor of the transformer, whose principle is similar to the phase-shift FBC.

## 3. FB-TPC for the Stand-Alone Renewable Power System

The FB-TPC, as shown in Fig.3, is applied to a stand-alone PV power system with battery backup to verify the topology. To better analyze the operation principle, the FB-TPC topology is redrawn in Fig.5, the two source ports are connected to a PV source and a battery respectively, while the output port is connected to a load.

There are three power flows in the standalone PV power system 1) from PV to load 2) from PV to battery and 3) from battery to load. As for the FB-TPC, the load port usually has to be tightly regulated to meet the load requirements, while the input port from the PV source should implement the

maximum power tracking to harvest the most energy. Therefore, the mismatch in power between the PV source and load has to be charged into or discharged from the battery port, which means that in the FB-TPC, two of the three ports should be controlled independently and the third one used for power balance. As a result, two independently controlled variables are necessary.

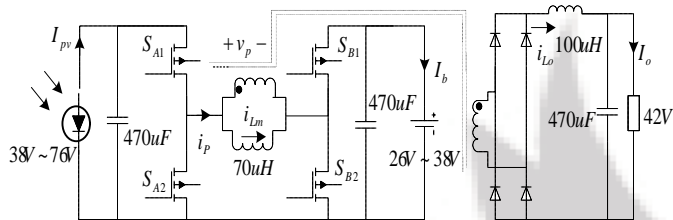


**Figure 5:** Topology of the FB-TPC

**A. Switching state analysis**

Ignoring the power loss in the conversion, we have

$$P_{pv} = p_b + P_o \tag{1}$$

where  $p_{pv}$ ,  $p_b$ , and  $p_o$  are the power flows through the PV, battery and load port, respectively. The FB-TPC has three possible operation modes 1) dual-output (DO) mode, with  $p_{pv} \geq p_o$  the battery absorbs the surplus solar power and both the load and battery take the power from PV 2) dual-input (DI) mode with  $p_{pv} \leq p_o$  and  $p_{pv} > p_o$ , the battery discharges to feed the load along with the PV and 3) single-input single-output (SISO) mode with  $p_{pv} = 0$ , the battery supplies the load power alone. When  $p_{pv} = 0$  exactly, the solar supplies the load power alone and the converter operate in a boundary state of DI and DO modes. This state can either be treated as DI or DO mode. Since the FB-TPC has a symmetrical structure, the operation of the converter in this state is the same as that of SISO mode, where the battery feeds the load alone. The operation modes and power flows of the converter are listed in Table I. The power flow paths/directions of each operation mode have been illustrated in Fig.6.

The switching states in different operation modes are the same and the difference between these modes are the value and direction of  $i_{Lm}$  as shown in Fig.5, which is dependent on the power of  $p_{pv}$  and  $p_o$ .

**Table 1:** Operation Modes of the FB-TPC

Operation modes	Power of PV	Power of battery
Dual-output mode	$p_{pv} \geq p_o$	Battery charging, $p_b \geq 0$
Dual-input mode	$p_{pv} \leq p_o, p_{pv} > 0$	Battery discharging, $p_b < 0$
Single-input single-output mode	$p_{pv} = 0$	Battery discharging, $p_b = p_o$

In the DO mode,  $i_{Lm}$  is positive, in the SISO mode,  $i_{Lm}$  is negative and in the DI mode,  $i_{Lm}$  can either be positive or negative. Take the DO mode as an example to analyse.

For simplicity, the following assumptions are made: 1)  $C_{pv}$ ,  $C_b$  and  $C_o$  are large enough and the voltages of the three ports,  $V_{pv}$ ,  $V_b$  and  $V_o$  are constant during the steady state and 2) the  $V_{pv} \geq V_b$  case is taken as an example for the switching state analysis.

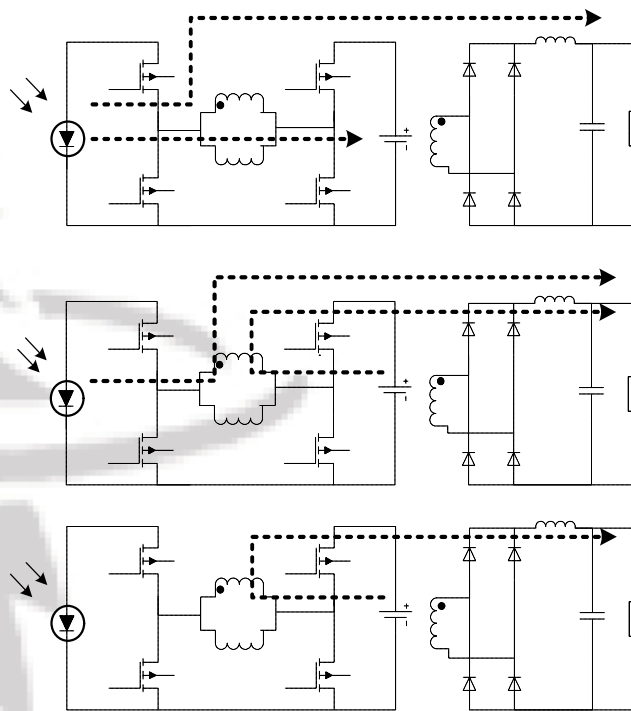


**Figure 6:** Power Flow Paths/Directions of each Operation Mode. (a) DO Mode. (b) DI Mode. (c) SISO Mode

There are four switching states in one switching cycle. The key waveforms are shown in Fig.11.

**State I [  $t_0 - t_1$  ]**

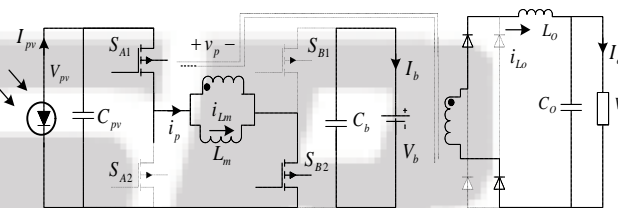


**Figure 7:** Equivalent Circuit of Switching State I [  $t_0 - t_1$  ]

Before  $t_0$ ,  $S_{A2}$  and  $S_{B2}$  are ON and  $S_{A1}$  and  $S_{B1}$  are OFF, while  $i_{Lm}$  freewheels through  $S_{A2}$  and  $S_{B2}$ . At  $t_0$ ,  $S_{A1}$  turns ON and  $S_{A2}$  turns OFF. A positive voltage is applied across the transformer's primary winding.

$$\left\{ \begin{array}{l} \frac{di_{Lm}}{dt} = \frac{V_{PV}}{L_m} \\ \frac{di_{Lo}}{dt} = \frac{nV_{PV} - V_O}{L_O} \\ i_p = i_{Lm} + ni_{Lo} \end{array} \right. \quad (2)$$

State II [ $t_1 - t_2$ ]

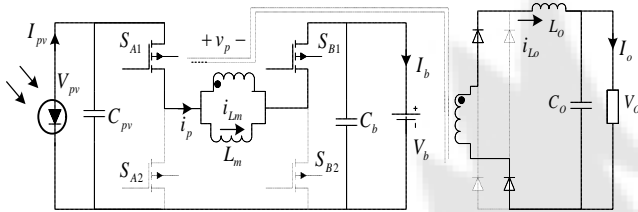


Figure 8: Equivalent Circuit of Switching State II [ $t_1 - t_2$ ]

At  $t_2$ ,  $S_{B2}$  turns OFF and  $S_{B1}$  turns ON. A positive voltage is applied on the primary winding of the transformer.

$$\left\{ \begin{array}{l} \frac{di_{Lm}}{dt} = \frac{V_{PV} - V_b}{L_m} \\ \frac{di_{Lo}}{dt} = \frac{n(V_{PV} - V_b) - V_O}{L_O} \\ i_p = i_{Lm} + ni_{Lo} \end{array} \right. \quad (3)$$

State III [ $t_2 - t_3$ ]

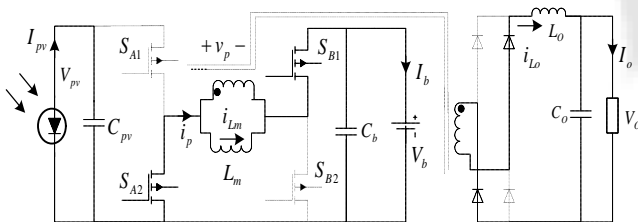


Figure 9: Equivalent Circuit of Switching State III [ $t_2 - t_3$ ]

At  $t_2$ ,  $S_{A1}$  turns OFF and  $S_{A2}$  turns ON. A negative voltage is applied on the primary winding of the transformer.

$$\left\{ \begin{array}{l} \frac{di_{Lm}}{dt} = -\frac{V_b}{L_m} \\ \frac{di_{Lo}}{dt} = \frac{nV_b - V_O}{L_O} \\ i_p = i_{Lm} - ni_{Lo} \end{array} \right. \quad (4)$$

State IV [ $t_3 - t_4$ ]

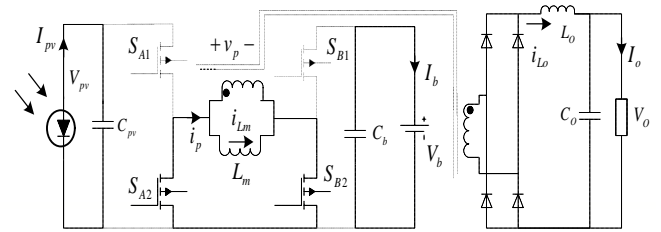


Figure 10: Equivalent Circuit of Switching State III [ $t_3 - t_4$ ]

At  $t_3$ ,  $S_{B1}$  turns OFF and  $S_{B2}$  turns ON. The voltage across the primary winding is clamped at zero and  $i_{Lm}$  freewheels through  $S_{A2}$  and  $S_{B2}$ .

$$\left\{ \begin{array}{l} \frac{di_{Lm}}{dt} = 0 \\ \frac{di_{Lo}}{dt} = \frac{-V_O}{L_O} \end{array} \right. \quad (5)$$

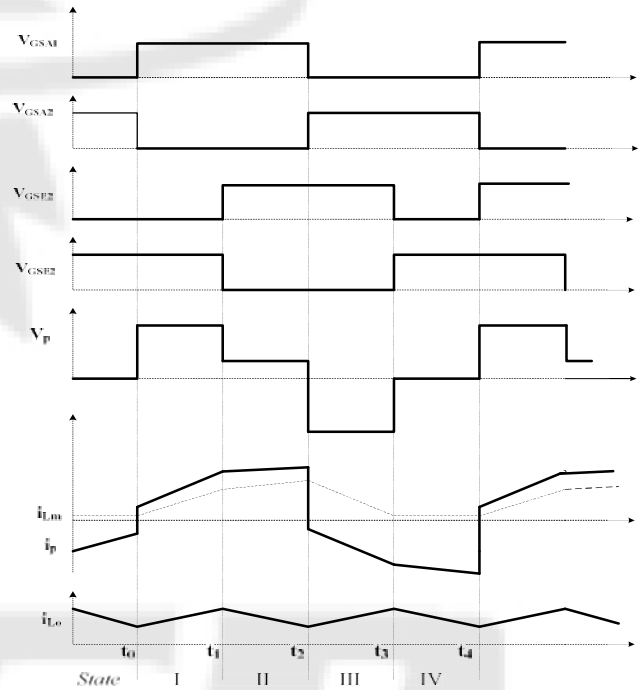


Figure 11: Key Waveforms of the FB-TPC

## B. Design Considerations

As for the semiconductor device stress, the FB-TPC is similar to the traditional FBC. But a key difference between these two converters is that the magnetizing inductance of the transformer  $L_m$  is operated as an inductor as well. We also take the  $V_{pv} \geq V_b$  case as an example for analysis. From (1), in the steady state, we have

$$V_{pv}I_{pv} = V_bI_b + V_oI_o \quad (6)$$

According to the switching states I and II, we have

$$I_{pv} = D_{A1}(I_{Lm} + nI_o) \quad (7)$$

where  $I_{Lm}$  is the average magnetizing current of the transformer, and then we have

$$I_{Lm} = \frac{I_{pv}}{D_{A1}} - nI_o \quad (8)$$

It can be seen that the larger the  $D_{A1}$ , the smaller the  $I_{Lm}$ . According to the switching states II and III, we have

$$\begin{aligned} I_b &= D_2(I_{Lm} + nI_o) - D_3(I_{Lm} - nI_o) \\ &= (D_{B1} - 2D_3)I_{Lm} + D_{B1}nI_o \end{aligned} \quad (9)$$

Then the average transformer magnetizing current  $I_{Lm}$  can also be given by the following equation:

$$I_{Lm} = \frac{I_b - D_{B1}nI_o}{D_{B1} - 2D_3} \quad (10)$$

$D_3$  is determined by  $V_b$  and  $V_o$ , therefore, the larger the  $D_{B1}$  the smaller the  $I_{Lm}$ . It is noticed that  $I_{Lm}$  can be reduced by increasing the nominal values of  $D_{A1}$  and  $D_{B1}$ ; this result is also valid for the  $V_{pv} < V_b$  case by following the same analysis procedure. Therefore, the value of  $I_{Lm}$  can be decreased with a properly designed modulation scheme.

#### 4. Simulation

Full bridge three port converter is simulated using MATLAB/SIMULINK. Simulink model of the Full Bridge Three Port Converter operating in dual output mode is shown in Fig.12.

Simulation of the full bridge three port converter operating in dual output mode is done by using 76V DC from PV array as input. A regulated voltage, 42V DC is obtained at the output side. The magnetizing inductor of the transformer performs buck operation. In closed loop system, the output will be fed back through the controller to the input. Carrier based PWM is used for the closed loop operation. Here R load is used as the load in the closed loop circuit. Hence if there is any over distortion or variation in results, the PWM technique will give the feedback to input according input varied. It gives better result compared to the open loop R load, because of stable result.

**Table 2:** Simulation Parameters of Full Bridge Three Port Converter

Input Voltage, $V_{in}$	38V~76V
Battery Voltage, $V_b$	26V~38V
Output Voltage, $V_o$	42V
Inductance, $L_o$	$100 \times 10^{-6}$ H
Leakage Inductance, $L_m$	$70 \times 10^{-6}$ H
Capacitance, $C_o$ , $C_b$ & $C_{pv}$	$470 \times 10^{-6}$ F
Resistor, $R$	9.82 $\Omega$
Switching Frequency, $F$	100 KHz

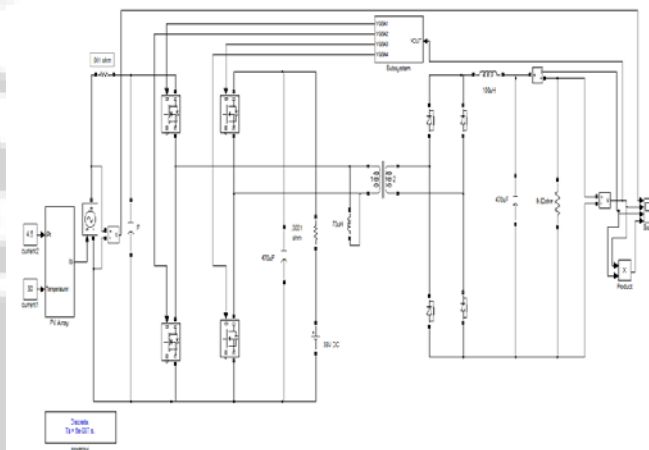


**Figure 12:** Simulink Model of the Full Bridge Three Port Converter for R load (closed loop)

In DO mode, the battery absorbs the surplus solar power and both the load and battery take the power from PV. It can be seen that, the output voltage, current and power of the converter are 42V, 4.3A and 180W respectively.

#### Input Voltage

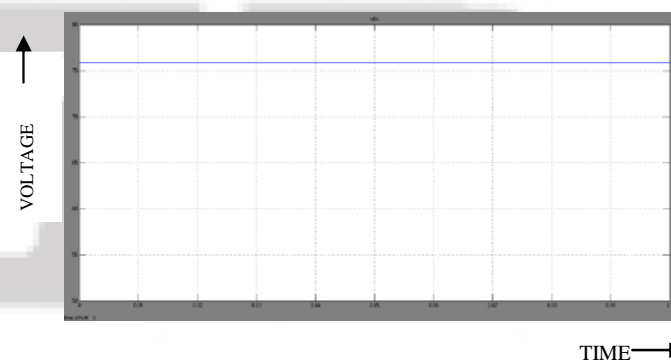


**Figure 13:**  $V_{IN} = 76V$ ( Input Voltage)



### Output Voltage

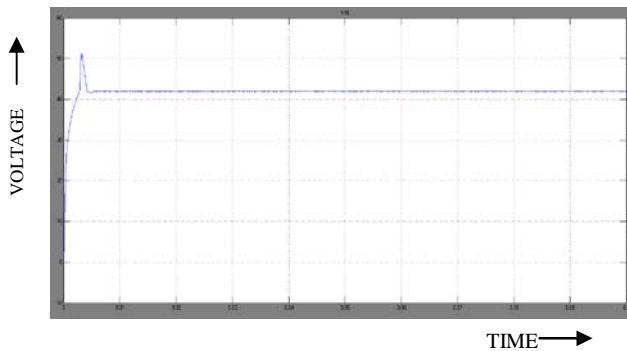


Figure 14:  $V_{OUT} = 42V$  (Output Voltage)

### Output Current

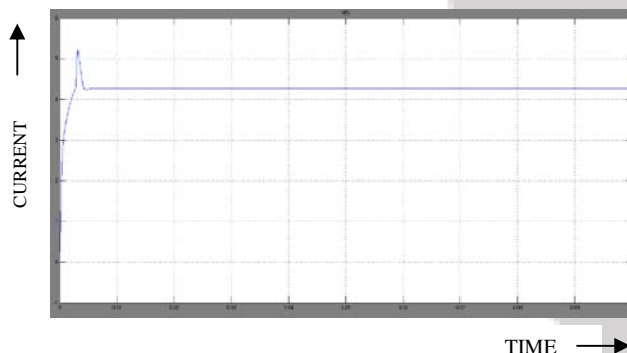


Figure 14:  $I_{OUT} = 4.3A$  (Output Current)

### Output Power

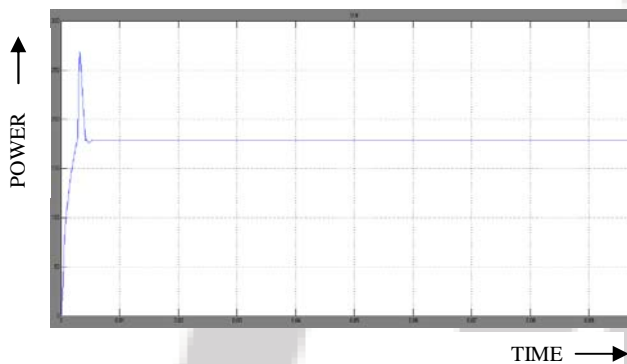


Figure 16:  $P_{OUT} = 180W$  (Output Power)

## 5. Conclusion

A Full-bridge converter generated with Three-port Full-bridges has been presented in this paper. A carrier based PWM control method is applied to the Three-port Full-bridge converter. The particular structure of a buck-boost Full-bridge, interfaces the port having a wide operating voltage, makes it possible to handle voltage variations at this port by adjusting the duty cycle of all the three Full-bridges. Carrier based

PWM scheme manages the power flow, regulates the output and adjusts the duty cycle in response to the varying voltage on the port. This converters offer the advantages of simple topologies and control, reduced number of devices and a single-stage power conversion between any two of the three ports. They are suitable for renewable power systems that are sourced by solar, thermoelectric generator etc with voltages varying over a wide range. Full bridge three port converter is simulated using MATLAB/SIMULINK validating the effectiveness of the converter and its control scheme. A 42V DC constant output is obtained for input voltage range 38V to 76 V DC.

## References

- [1] W. Jiang and B. Fahimi, "Multi-port power electric interface for renewable energy sources," in *Proc. IEEE Appl. Power Electron. Conf.*, 2009, pp. 347–352.
- [2] W. Jiang and B. Fahimi, "Multiport power electronic interface—Concept, modeling and design," *IEEE Trans. Power Electron.*, vol. 26, no. 7, pp. 1890–1900, Jul. 2011.
- [3] H. Tao, J. L. Duarte, and M. A. M. Hendrix, "Multiport converters for hybrid power sources," *IEEE Proc. Power Electron. Spec. Conf.*, pp. 3412–3418, 2008.
- [4] H. Tao, A. Kotsopoulos, J. L. Duarte, and M. A. M. Hendrix, "Family of multiport bidirectional dc-dc converters," *Inst. Electr. Eng. Proc. Elect. Power Appl.*, vol. 153, no. 15, pp. 451–458, May 2006.
- [5] Z. Qian, O. Abdel-Rahman, H. Al-Atrash, and I. Batarseh, "Modeling and control of three-port DC/DC converter interface for satellite applications," *IEEE Trans. Power Electron.*, vol. 25, no. 3, pp. 637–649, Mar. 2010.
- [6] Z. Qian, O. Abdel-Rahman, H. Hu, and I. Batarseh, "An integrated threeport inverter for stand-alone PV applications," presented at the *IEEE Energy Convers. Congr. Expo*, Atlanta, GA, 2010.
- [7] H. Wu, R. Chen, J. Zhang, Y. Xing, H. Hu, and H. Ge, "A family of threeport half-bridge converters for a stand-alone renewable power system," *IEEE Trans. Power Electron.*, vol. 26, no. 9, pp. 2697–2706, Sep. 2011.
- [8] C. Zhao, S. D. Round, and W. Johann, "An isolated three-port bidirectional DC-DC converter with decoupled power flow management," *IEEE Trans. Power Electron.*, vol. 23, no. 5, pp. 2443–2453, Sep. 2008.
- [9] J. L. Duarte, M. A. M. Hendrix, and M. G. Simoes, "Three-port bidirectional converter for hybrid fuel cell systems," *IEEE Trans. Power Electron.*, vol. 22, no. 2, pp. 480–487, Mar. 2007.
- [10] H. Al-Atrash and I. Batarseh, "Boost-integrated phase-shift full-bridge converter for three-port interface," in *Proc. IEEE Power Electron. Spec. Conf.*, 2007, pp. 2313–2321.
- [11] S. Waffler and J. W. Kolar, "A novel low-loss modulation strategy for high-power bidirectional Buck+Boost converters," *IEEE Trans. Power Electron.*, vol. 24, no. 6, pp. 1589–1599, Jun. 2009.